JMEPEG (2011) 20:1544–1553
DOI: 10.1007/s11665-011-9836-0

1059-9495/$19.00

Optical Film for LED with Triangular-Pyramidal Array Using Size-Reducible Embossing Method

C.F. Liu, C.T. Pan, K.H. Liu, Y.C. Chen, J.L. Chen, and J.C. Huang

(Submitted March 3, 2010; in revised form October 27, 2010)

This study presents a modified hot-embossing process to fabricate micro-triangular-pyramidal array (MTPA). First, a tungsten (W) steel mold (as the first mold) is manufactured by precision machining including optical projection grinding, lapping, and polishing processes. The dimension of a triangular pyramid with acute angle of 85° on the W-steel mold is about 300 μm in width and 139 μm in height. The pitch between two triangular-pyramidal tips is about 170 μm. Then, only the portion of the tip area of the triangular-pyramidal patterns is transferred on bulk metallic glass (BMG, $Mg_{58}Cu_{31}Y_{11}$) using this modified multi-step hot-embossing method to reduce the pattern size. With a position-adjustable mechanism, size-reduced concaved-shaped MTPA can be selectively formed, used as the secondary mold. In this way, not only can the size of triangular-pyramidal patterns on W-steel mold be reduced down on BMG, but also the tool arc between each triangular-pyramid on W-steel mold caused by machine tool can be eliminated. This is based on the fact that amorphous glass alloys contain no dislocation that can be responsible for yielding in crystalline materials. Thus, BMG is expected to be strong and hard enough to be used as a mold material. Then the secondary mold is used to emboss convex-shaped MTPA on PolymethylMethacrylate (PMMA) optical film. Experiments with different embossing times and embossing pressures are conducted and discussed. Large-sized triangular-pyramidal array on the W-steel mold has been successfully and selectively miniaturized on BMG, and then transferred on PMMA. Finally, this optical film of PMMA with MTPA is packaged on light-emitting diode (LED) to improve its lighting uniformity and luminance. In comparison with commercial 3M™ optical film (3M™ Vikuiti™ TBEF2-T-65i), the film with MTPA shows a good optical performance.

Keywords BMG, hot embossing, multi-step, optical film, size-reducible, triangular-pyramidal

1. Introduction

In recent years, micro-optical elements have been gaining a lot of attention by researchers due to their wide applications in the fields of optical communication, optical storage, and digital displays. Among these applications, integrated microstructure array plays an important role in micro-optical components such as video cameras, video phones, optical scanners, and high-definition projection displays. The major objective of optical film, such as micro-lens arrays, is to increase the coupling efficiency of optical system, to enhance the brightness of backlight module (BLM) for liquid crystal display (LCD) and to increase the efficiency of optical switches. For instance, Ezell (Ref 1) applied micro-lens technology to enhance optical intensity output in a laptop display.

Many fabrication methods of refractive micro-lens were reported (Ref 2-13), and most of which used photoresist reflow technique (Ref 2-7). Some micro-optical components were fabricated by molding (either hot embossing or injection molding) (Ref 14-16). In addition, deep x-ray lithography was used to fabricate micro-optical components (Ref 17). Other methods, such as the contraction effect of UV-curable photopolymers method (Ref 18), excimer laser micromachining method (Ref 19), and focused ion beam (FIB) milling method (Ref 20) were also used to fabricate micro-lens array. The cost of synchrotron radiation facility is considerably more than ultraviolet (UV) exposure system. In addition, hot-embossing technology can offer a low cost process to form circular micro-lens array (Ref 21).

In general, microstructure array fabricated on optical film was used to increase efficiency of optical system, such as the optical films reported by Kim (Ref 22, 23) and Chang and Fang (Ref 24) for LCD backlight. In addition, optical films with micro-lens array were combined with light-emitting diode (LED) to improve brightness and chroma (Ref 25). Furthermore, the films were used to maximize the directivity of the output beam of LEDs, to optimize the external quantum efficiency, and to focus the light on a spot at a certain distance (Ref 26). Thus, it can be seen that an optical film plays an important role in the development of LED.

This study presents a modified hot-embossing method to fabricate micro-triangular-pyramidal arrays (MTPA). For optical function, when the light passes through the optical film with

C.F. Liu and **K.H. Liu**, Department of Mechanical Engineering, R.O.C. Military Academy, Kaohsiung, Taiwan, R.O.C; **C.T. Pan, Y.C. Chen,** and **J.L. Chen**, Department of Mechanical and Electro-Mechanical Engineering, and Center for Nanoscience & Nanotechnology, National Science Council Core Facilities Laboratory for Nano-Science and Nano-Technology in Kaohsiung-Pingtung area, National Sun Yat-Sen University, Kaohsiung, Taiwan 804; and **J.C. Huang**, Institute of Materials Science & Engineering, Center for Nanoscience and Nanotechnology, National Sun Yat-Sen University, Kaohsiung, Taiwan 804. Contact e-mail: panct@mail.nsysu.edu.tw.

MTPA, it would be expected to improve the intensity and uniformity. Combined with a precision machining method, a tungsten (W) steel mold with triangular-pyramidal array is manufactured by optical projection grinding, lapping, and polishing. Then, the triangular-pyramidal array is transferred on bulk metallic glass (BMG) to form a smaller MTPA. Selection of BMG as mold material is based on the fact that amorphous alloys contain no dislocation that can be responsible for yielding in crystalline materials, and are therefore expected to be strong and hard (Ref 27-32). Then using a modified multi-step hot-embossing method with position-adjustable mechanism, a more miniaturized concaved-shaped MTPA than the original one on W-steel mold can be formed on $Mg_{58}Cu_{31}Y_{11}$ of BMG material. The BMG material is used as a secondary mold. Then with this mold, a convex-shaped MTPA is embossed on PolymethylMethacrylate (PMMA) sheet using this modified multi-step hot-embossing process. In addition, Photo research 650 (PR-650) is used for optical measurement. The MTPAs were fabricated on a polymer film, called an optical film, and were tested by Spectra Scan Colorimeter PR-650 (Photo Research, Inc., Chatsworth, CA, USA). The measurement set-up was controlled by a computer, including a test sample and a power supply. It can measure the luminance of a light source. A clamping apparatus is mounted on *X-Y-Z* table which can move at specific distance. A power supply (2400 Source Meter, Keithley) can provide DC (direct current) to an optical film as a light source in this measurement. The optical characteristics of this optical MTPA-PMMA film such as uniformity and luminance are compared with those of the commercial 3M™ optical film (3M™ Vikuiti™ TBEF2-T-65i) to realize its optical performance.

2. Optical Function for Triangular Pyramid

When incident light passes through a MTPA, light reflection and then refraction can happen on the opposite surface. As a result, the light propagates toward the direction of observer after reflection. In our laboratory, a gapless triangle microlens arrays have been fabricated and studied (Ref 33). The result shows that triangle microlens is better than spherical one. Thus, pattern of triangle microlens array is a good choice for optical film. In addition, the design of micro-triangular pyramid array is inspired by the module of 3M™ BEF. When two pieces of 3M films are stacked relative to 90°, the projection of the stacked pattern looks like a pyramidal structure. Therefore, based on the concept, the design and fabrication of the micro-triangular pyramid is conducted. The preliminary result shows that the film with triangle microlens can be comparable with that of 3M. It shows potential in the BEF application.

For a single incident light, the optical function of two neighbor micro-triangular-pyramidal structures is illustrated in Fig. 1. The refraction and reflection happen at both interfaces, which depend on the critical angle, Fresnels equations, and the refractive index of the PMMA material. It shows the predicted light path, including an incident angle of θ_a, a refractive angle of θ_b, and a reflective angle of θ_c. For this reason, MTPA is fabricated in the study. In this study, Fig. 1 is a schematic projection of the front view. It only shows the propagation of light ray schematically. Since most fabrications of optical film are restricted by the 3M™ patents, this study aims at how to create a new film, but comparable with 3Ms. Before fabrication process, micro-triangular pyramid arrays were simulated. At first, the various apex angles of triangular pyramid such as 80°, 85°, and 90° were simulated using FRED commercial optical software. The result shows that triangular pyramid with 85° exhibits better optical performance. Based on the simulation result, the mold is fabricated using mechanical cutting method. With this mold, the optical thin film can be made.

3. Process Procedures

3.1 Multi-Step Hot-Embossing Concept

In this study, we present a modified hot-embossing process to fabricate MTPA as schematically shown in Fig. 2. The schematic illustration of multi-step hot-embossing process is shown in Fig. 2(a). It is worth noticing that there could be a tool arc left behind after precision machining. The arrangement of patterns on the W-steel mold is shown in Fig. 2(b). First, the W-steel mold (as the first mold) with the triangular-pyramidal patterns is embossed on BMG for the first step hot-embossing process as shown in Fig. 2(c). With position-adjustable mechanism, the second step hot-embossing process is performed. If more steps are taken, then a denser and more complicated pattern can be formed. In this study, only a two-step embossing process is demonstrated. In this way, a smaller concaved-shaped MTPA without tool arc is formed using this modified multi-step hot-embossing method as shown in Fig. 2(d).

Then the BMG mold (used as the secondary mold) shown in Fig. 2(d) is used to emboss convex-shaped MTPA on PMMA. As a result, using this multi-step hot-embossing process, triangular-pyramidal patterns on the W-steel mold can be successfully miniaturized on BMG, and then transferred on PMMA. Furthermore, MTPA with different sizes and densities

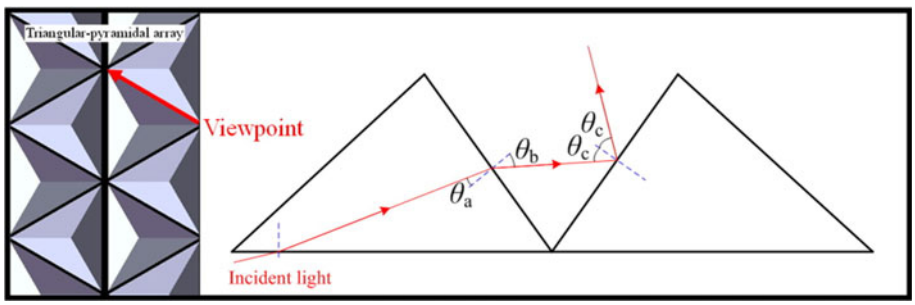

Fig. 1 Schematic illustration of optical function for the neighbor triangular-pyramidal structures

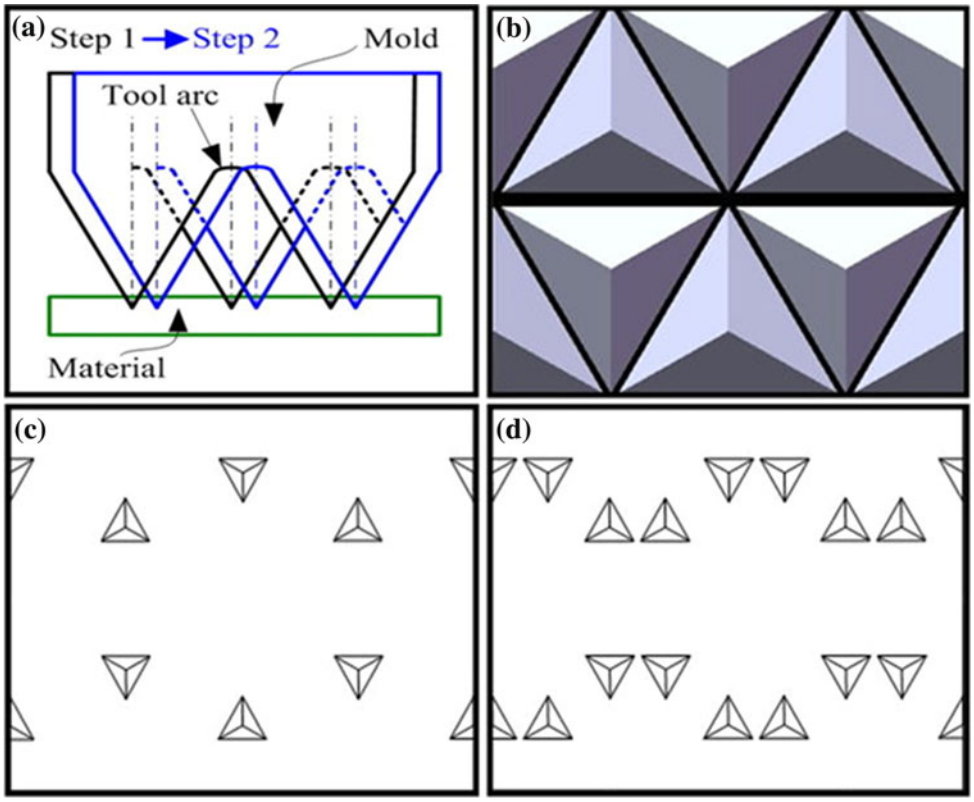

Fig. 2 The schematic illustration of (a) multi-step hot-embossing process using (b) the W-steel mold and the patterns after (c) one step hot-embossing process, and (d) the miniaturized and compact micro-triangular-pyramidal tip array can be obtained by the concept of multi-step imprint

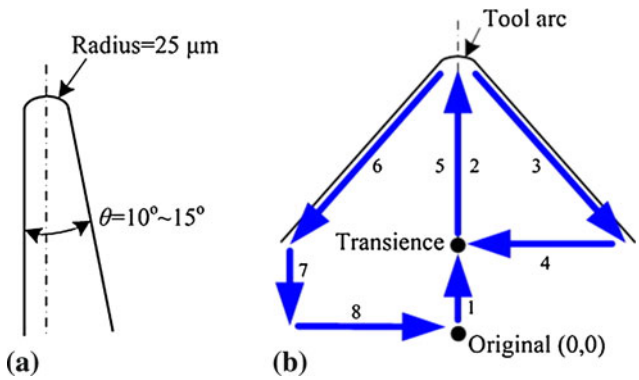

Fig. 3 The tool (a) with a radius of 25 μm and an angle of 10°-15° is used to manufacture the triangular-pyramidal shape following (b) the path from 1 to 8

can be readily formed with just a single mold, which can be more cost-effective.

3.2 W-Steel Mold Manufacture

Precision machining, including computer numerical control (CNC) optical projection grinding, lapping, and polishing, is employed to fabricate a W-steel mold with triangular-pyramidal patterns. A diamond grinding wheel of knife type is used in this study. The radius of tool is 25 μm as shown in Fig. 3(a), which will cause tool arc. The tool path of manufacture for a triangular pyramid is schematically shown in Fig. 3(b). In this current design, the dimension and geometric relationship of the triangular pyramid is schematically illustrated in Fig. 4. The slanted surfaces of the triangular pyramids can be fabricated with assistance of punch grinders. For a single triangular pyramid shown in Fig. 4(b), the dimensions are defined as values of length (L), centerline (D), and taper angle (θ) of the W-steel tip and a tip-to-tip spacing (G) as shown in Fig. 4(c).

4. Results and Discussions

4.1 W-Steel Mold with Triangular-Pyramidal Array

Figure 5(a) shows the scanning electron microscopic (SEM) images of W-steel mold with triangular-pyramidal array. From the SEM image, the dimensions of length (L) and centerline (D) are about 300 and 173 μm, respectively. In addition, a tip-to-tip pitch (G) of two neighbor triangular pyramids is about 170 μm. Based on the taper angle of the W-steel tip of 85° (θ, see Fig. 4b), the height of the W-steel mold is about 139 μm. From the result, the W-steel mold with triangular-pyramidal patterns can be fabricated by precision machining. Nevertheless, the tool arcs are caused as shown in Fig. 5(b) as a result of the tool radius of 25 μm during precision machining process.

4.2 One-Stepped Hot-Embossing Process

To demonstrate the proposed hot-embossing process, the W-steel mold is used to emboss on BMG in one-stepped forming process with a constant load of 36.06 N for 2-9 min.

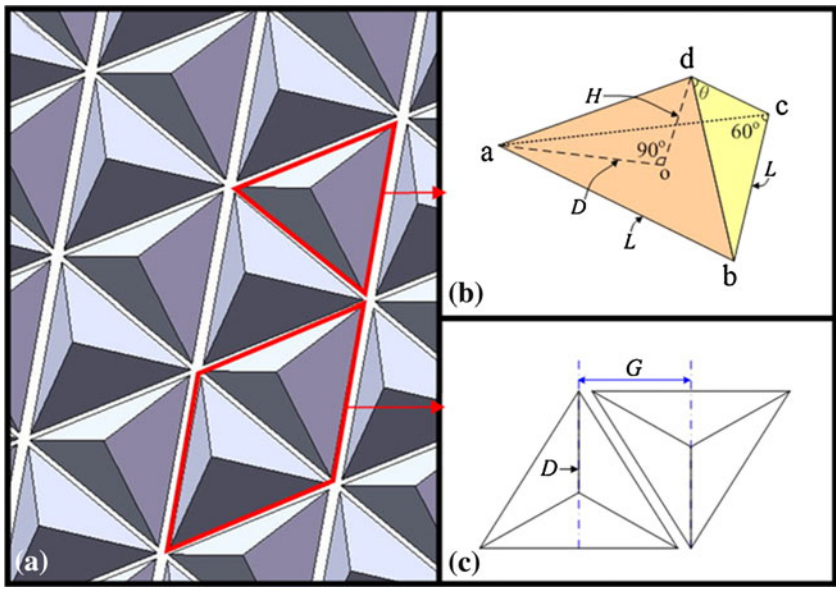

Fig. 4 The schematic illustration of (a) the triangular pyramid array and the dimension and geometric relationship of (b) a single triangular pyramid with the dimensions of L, D, and θ and (c) the horizontal pitch, G, of two neighbor triangular pyramids on the wolfram steel mold

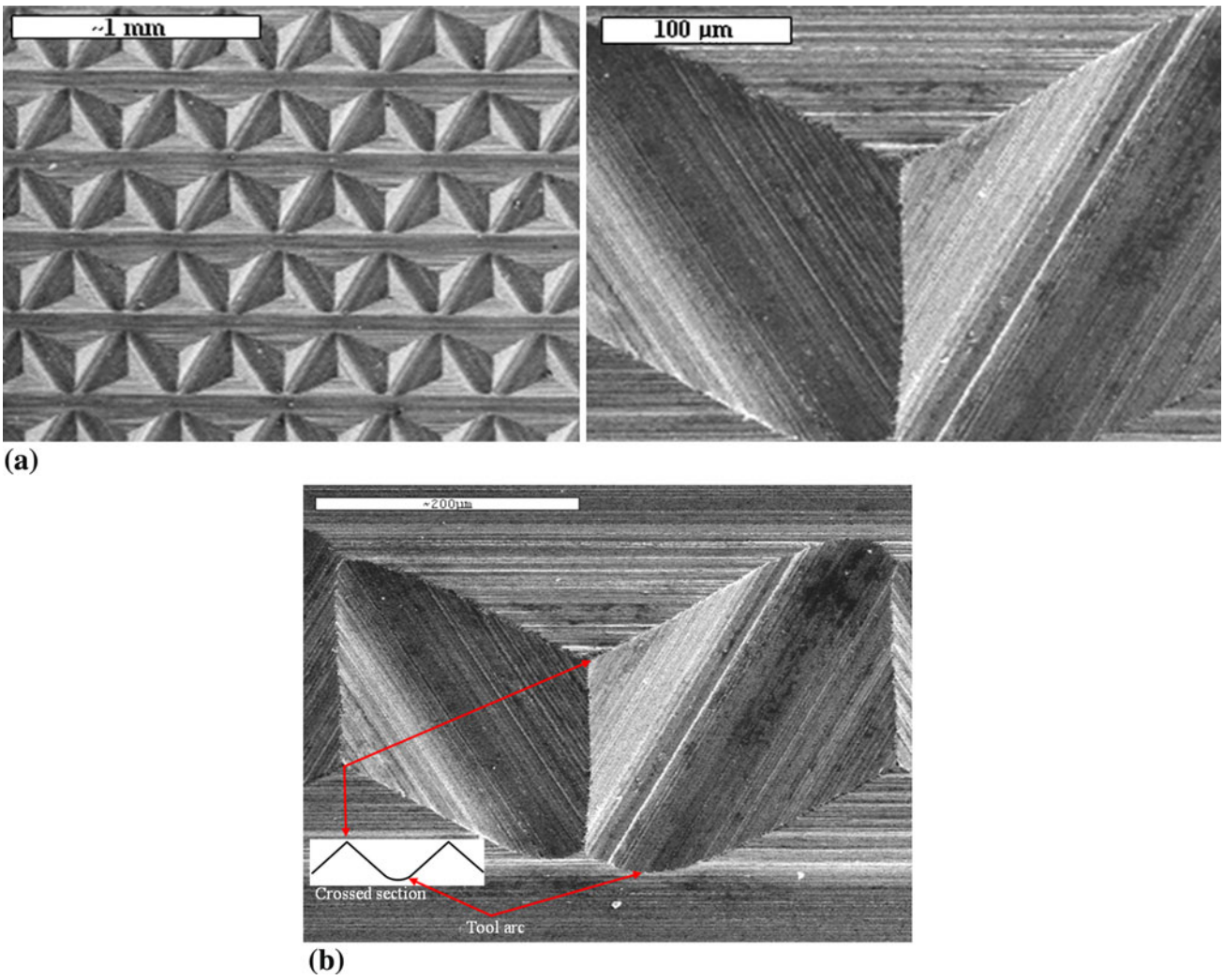

Fig. 5 SEM photos of (a) triangular-pyramidal micro-array and (b) a single triangular pyramid on the wolfram steel mold (convex-shaped)

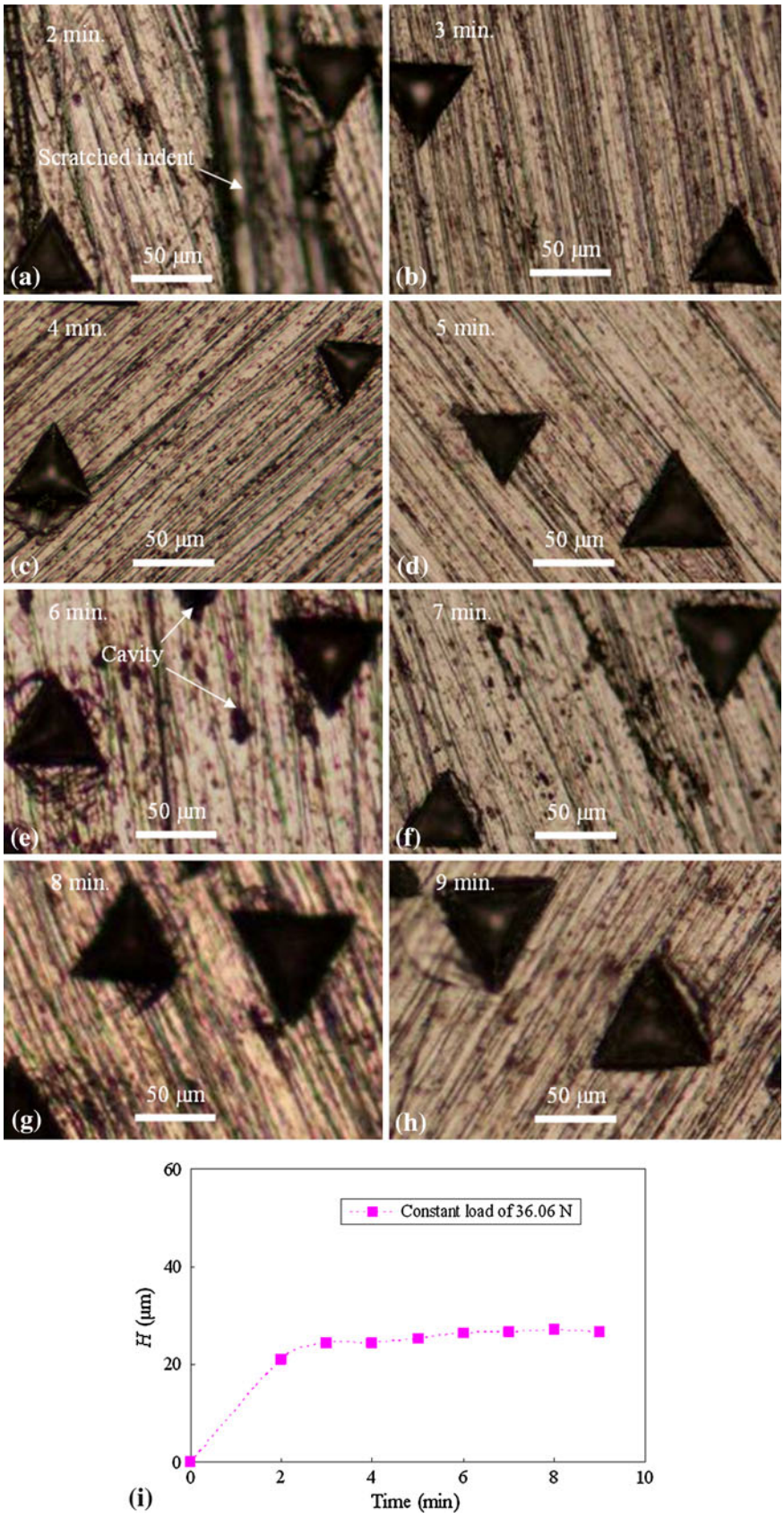

Fig. 6 One-stepped hot-embossing process using the wolfram steel mold is carried out on BMG (concaved-shaped) with constant load of 36.06 N and for different time (a) to (h) 2 to 9 min, respectively, and (g) the height (H) as a function of embossing time

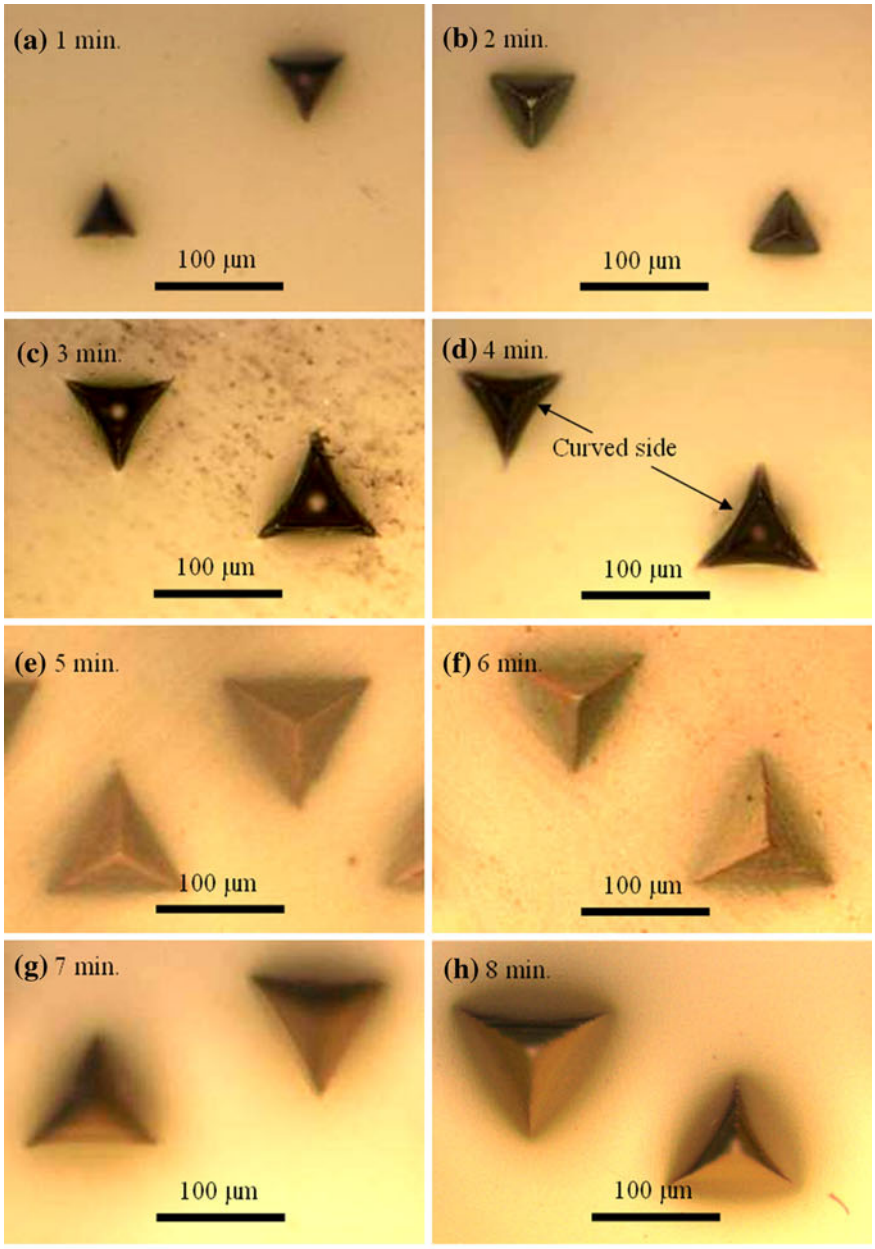

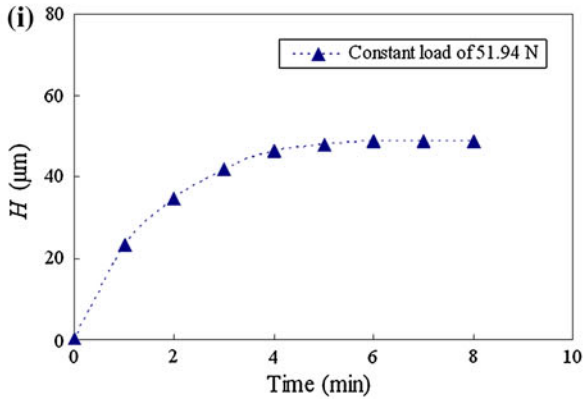

Fig. 7 One-stepped hot-embossing process using the W-steel mold is carried out on PMMA sheet (concaved-shaped) under a constant load of 51.94 N and for different times (a) to (h) 1 to 8 min, respectively, and (g) the height (*H*) as a function of embossing time

The concaved-shaped patterns can be transferred on BMG after one-stepped hot-embossing process and the triangular patterns are shown in Fig. 6(a) to (h). Also, the embossed depths of the BMG patterns as a function of embossing time are shown in Fig. 6(g). It reveals that the embossing is going to approach saturation, and the dimension of triangular-pyramidal patterns is reaching stable. It takes about 3-4 min to complete a successful embossing process. It can be seen clearly that there are some marks, such as residual scratched indent and cavities, as shown in Fig. 6(a) or (e) on the surface of a BMG raw material, which was produced during its manufacturing process. To improve this, the surface was polished with abrasive papers of No. 2000. However, parallel bands and marks on the surface are observed clearly in Fig. 6(a) to (h) after embossing.

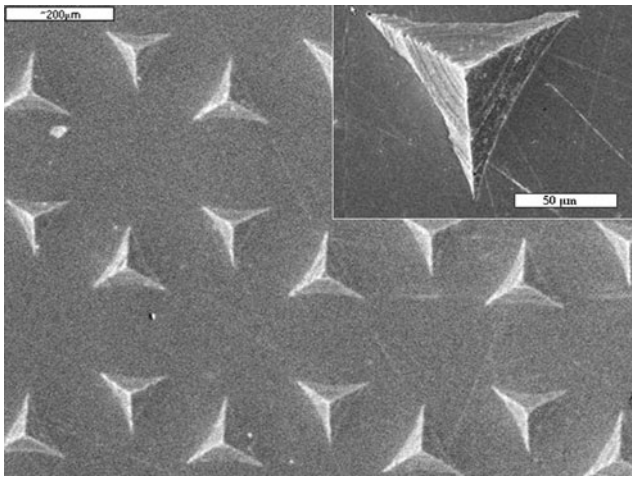

Fig. 8 SEM photos of the micro triangular-pyramidal array on PMMA (concaved-shaped) using one-stepped hot-embossing testing with constant load of 51.94 N for 5 min

On the other hand, to realize the characteristics of PMMA, similar experiments are performed on PMMA under a constant load of 51.94 N for 1-8 min, the W-steel mold is used to emboss on PMMA sheets in one-stepped forming process with a constant load of 51.94 N for 1-8 min. For a constant load, the sizes of the formed patterns (concaved-shaped) are shown in Fig. 7(a) to (h). However, in Fig. 7(c) and (d), it can be seen that some of the formed patterns have curved sides due to insufficient embossing time, which influences the qualities of patterns transferred. For the thermal expansion of PMMA, below the glass transition temperature (T_g) of about 120 °C, a thermal expansion coefficient (α) of $(75 \pm 25) \times 10^{-6}$ m/mK was reported (Ref 34). Thus, to reduce the influences of thermal expansion on the forming process, the embossed material should be held under a constant pressure until the temperature is cooled down to room temperature. The embossed depths of the PMMA patterns are shown in Fig. 7(g). It reveals that the embossing is going to approach saturation, and the dimension of triangular-pyramidal patterns is reaching stable. It takes about 4-5 min to complete a successful embossing process. Figure 8 shows the SEM photos of the triangular-pyramidal array on PMMA (concaved-shaped) using one-stepped hot-embossing testing with constant load of 51.94 N for 5 min.

Compared with the patterns in Fig. 7(a) to (h), most of the patterns shown in Fig. 6(a) to (h) have straight sides. It may be

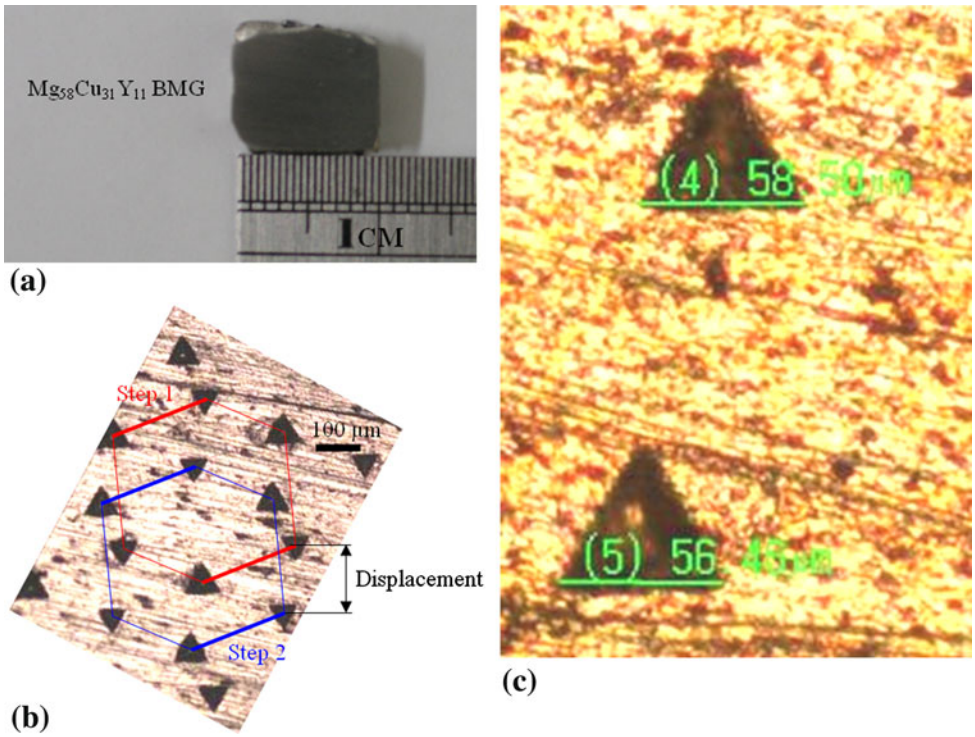

Fig. 9 (a) On the $Mg_{58}Cu_{31}Y_{11}$ BMG, (b) the minified concaved-shaped micro triangular-pyramidal array is formed using a two-stepped hot-embossing method with the W-steel mold and a position-adjustable mechanism for a displacement of about 150 μm, and (c) triangular pyramids have an average side (L_1) of about 55.1 μm

for two reasons. One reason is that the embossed material BMG is held under a constant pressure until the temperature is cooled to room temperature in hot-embossing process; the other is that for the $Mg_{58}Cu_{31}Y_{11}$ BMG, below its T_g of about 140 °C, a low linear thermal expansion coefficient (α) of $(3 \pm 1) \times 10^{-6}$ m/mK was reported (Ref 27). In addition, having a good glass-forming ability (GFA), the dimension of triangular-pyramidal patterns on the $Mg_{58}Cu_{31}Y_{11}$ BMG is going to approach stable value, which is shown in Fig. 6(g), under a smaller pressure than that pressed on the PMMA sheet, which is shown in Fig. 7(g).

Therefore, we believe that the triangular-pyramidal patterns can be successfully transferred on BMG or on PMMA using the W-steel mold. In this case, most of the applied pressure and mold deformation could be focused on the W-steel mold tips. It is necessarily to choose a properly hot-embossing force to avoid damaging the mold. Referring to the above experiments, a force smaller than 36.06 N is high enough for BMG forming. Based on Fig. 6(g), a proper force can be chosen for multi-stepped hot-embossing process on BMG.

4.3 Multi-Step Hot-Embossing Process

4.3.1 The Secondary Mold, BMG Mold. Two-stepped hot-embossing method was applied on the $Mg_{58}Cu_{31}Y_{11}$ BMG (see Fig. 9(a)) with a displacement of 150 μm to fabricate a secondary mold. The stepped displacement is defined as the distance between two different embossing movements. The displacement is shown in Fig. 9(b). In Fig. 9(b), a miniaturized MTPA has been embossed on BMG using the W-steel mold. The patterns in the area surrounded by red lines are the patterns embossed in step 1 and those surrounded by blue lines is embossed in step 2; thus, with an appropriate force and displacement during the hot-embossing process, patterns without overlapping can be fabricated. With the multi-step hot-embossing concept, in addition to miniaturized MTPA, the tool arc between each triangular-pyramid in the first mold caused by machine tool can also be avoided. The BMG mold (see Fig. 9b) considered as a secondary mold is used to emboss convex-shaped MTPA on PMMA.

4.3.2 Convex PMMA Microstructures. In Fig. 10(a), using the BMG mold with MTPA as the secondary mold, the convex-shaped MTPA (see Fig. 10b) can be transferred on PMMA sheet. Nevertheless, the shrinkage (δ) phenomena exist due to the thermal expansion. The rough estimation of shrinkage is calculated by comparing the lateral lengths of the pyramid between the BMG material and the PMMA material. Figure 9(c) shows that the patterns on BMG have an average side (L_1) of about 57.5 μm, while the patterns on PMMA sheet have an average side (L_2) of about 55.3 μm as shown in Fig. 10(c); thus, the δ, which is defined as $|(L_1 - L_2)|/(L_1)$, is estimated to be around 0.038, about 3.8%.

The concept of multi-step embossing process has been carried out in this study. However, in the two-stepped hot-embossing process, there are some p problems that need to be addressed. Firstly, the position accuracy is difficult to control because the high temperature condition and embossing force may affect the positioning accuracy of position-adjustable mechanism, which should be improved in the future study. Secondly, in Fig. 9(b) and 10(b), the patterns of step 1 are slightly different from that of step 2. The variation may be due to thermal reflow and compression effect, which could affect the embossed result in the first step.

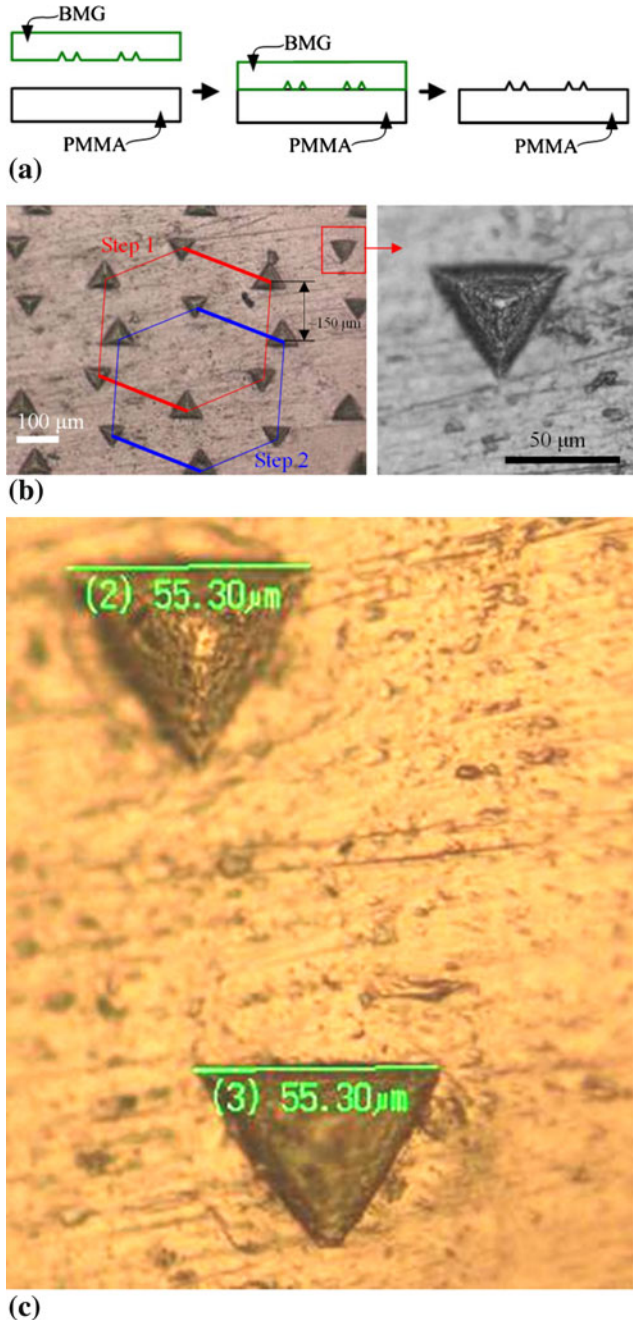

Fig. 10 (a) Using the BMG mold as the secondary mold for a hot-embossing process, (b) the convex-shaped MTPA can be transferred on PMMA sheet; (c) triangular pyramids have an average side (L_2) of about 51.4 μm

4.4 Optical Measurement

In order to realize optical characteristics such as luminance and uniformity, the optical film are measured using PR-650. A LED (light emitting diode; 1505 White SMD LED, LT-15056C1-WD-CA1-0A) of lampshade is used as a light source. It is packaged with the optical film with MTPA. The test result of sample one to three is shown in Fig. 11. Figure 11(a) shows an optical instrument, PR-650, used to measure the optical properties such as luminance and uniformity for these samples. The sample No. 1 is an optical film without any pattern on PMMA film, used as reference film; the sample No. 2 is a purchased 3M™

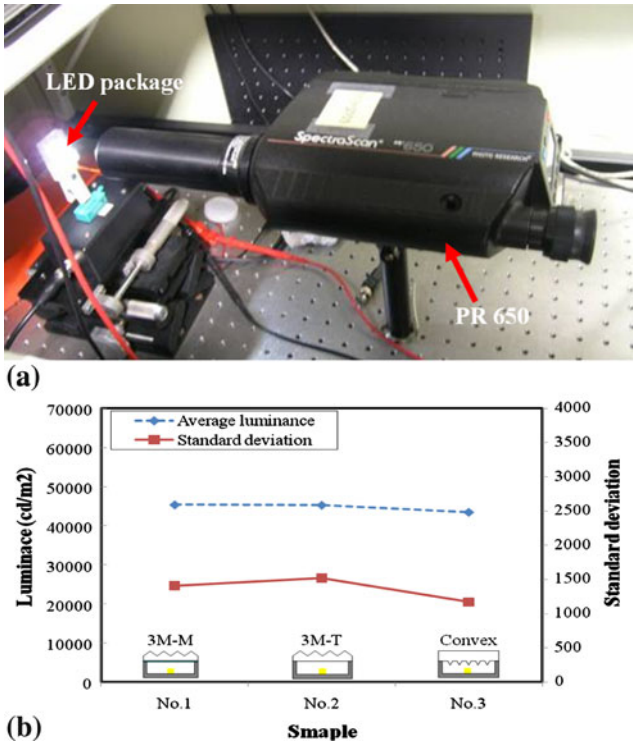

Fig. 11 (a) A optical instrument, PR-650, are used to measure the optical properties like (b) luminance and uniformity for the samples: No. 1, a purchased $3M^T$ optical film, and No. 2, a purchased $3M^M$ optical film, and No. 3, this study

optical film (from 3M™ Vikuiti™ TBEF2-T-65i), which has been widely used in back light module (BLM) package for thin film transistor liquid crystal display (TFT LCD); and the sample No. 3 is a sample fabricated according to the process mentioned in section 4.3.2. Compared to the optical thin film of 3M™ as illustrated in Fig. 11(b), The authors made some mistakes in the luminance of blank PMMA. To have clear understanding for reader, the graph was re-arranged. $3M^T$, $3M^M$ brightness enhancement film (BEF) and ours are compared. No. 1 and No. 2 are optical films from $3M^T$ and $3M^M$, respectively. The result shows that the luminance of $3M^T$ and $3M^M$ are larger than that of ours (No. 3). However, the standard deviation of No. 3 is better than those of $3M^T$ and $3M^M$. Figure 11(b) shows the optical luminance and standard deviation of samples; No. 1 is 45400 cd/m^2 and 1410; and No. 2 is 45300 cd/m^2 and 1520; No. 3 is 43200 cd/m^2 and 1170, respectively. When the value of standard deviation is smaller, it means that the variation of brightness in the nine points is less; thus, the uniformity is better. The commercial product of 3M™ BEF is used predominantly for back light module. 3M holds this key patent. In this study, the optical film with micro-triangular pyramid array can really enhance the luminance, which is comparable with 3M™ BEF, but a little less than that of 3M. Thus, this optical film can be fabricated using this multi-step size-reducible hot-embossing process, and shows a potential to substitute for 3M™ thin films for LED package.

5. Conclusion

Micro-triangular-pyramidal array has successfully fabricated in this study. Using the W-steel tips array, micro-triangular-pyramidal arrays with different sizes and densities can be readily formed with a single mold. Furthermore, with the concept of the secondary mold, convex-shaped micro-triangular-pyramidal array is transferred on PMMA optical film. Thus, concave- or convex-shaped microstructures can be formed by the new multi-step hot-embossing process. Though the luminance decreases due to a medium absorption effect, the variation relative to the initial light can be controlled below 15%. In addition, the uniformity improved by this optical MTPA-PMMA film shows a good optical performance when compared to that of the commercial 3M™ optical film. This technique is expected to provide a simple, efficient, and low-cost method to create variable micro-arrays for optical application.

Acknowledgments

The authors would like to thank National Science Council (NSC) for their financial supports to the project (granted number: NSC97-2622-E-110-002-CC3). Also, the authors would like to thank the Center for Nanoscience & Nanotechnology, National Sun Yat-Sen University, Kaohsiung, Taiwan, for equipment access and technical support.

References

1. B. Ezell, Making Micro-Lens Backlights Grow Up, *Inf. Disp.*, 2001, **5**, p 42–45
2. Z.D. Popovic, R.A. Sprague, and G.A.N. Connell, Technique for the Monolithic Fabrication of Micro-Lens Arrays, *Appl. Opt.*, 1988, **27**, p 1281–1284
3. M.C. Hutley, Optical Techniques for the Generation of Micro-Lens Arrays, *J. Mod. Opt.*, 1990, **37**, p 253–265
4. J.O. Choi, J.A. Morse, J.C. Corelli, J.P. Silverman, and H. Bakhru, Degradation of poly(methylmethacrylate) by Deep Ultraviolet, X-ray, Electron Beam, and Proton Beam Irradiations, *J. Vac. Sci. Technol. B*, 1988, **6**, p 2286–2289
5. N.F. Borrelli, D.L. Morse, R.H. Bellman, and W.L. Morgon, Photolytic Technique for Producing Micro-Lenses in Photosensitive Glass, *Appl. Opt.*, 1985, **24**, p 2520–2525
6. H. Yang, C.-K. Chou, M.-K. Wei, and C.P. Lin, High Fill-Factor Micro-Lens Array Mold Insert Fabrication Using a Thermal Reflow Process, *J. Micromech. Microeng.*, 2004, **14**, p 1197–1204
7. C.P. Lin, H. Yang, and C.K. Chou, Hexagonal Micro-Lens Array Modeling and Fabrication Using a Thermal Reflow Process, *J. Micromech. Microeng.*, 2003, **13**, p 775–781
8. L. Kong, X. Yi, K. Lian, and S. Chen, Design and Optical Performance Research of Multi-Phase Diffractive Micro-Lens Arrays, *J. Micromech. Microeng.*, 2004, **14**, p 1135–1139
9. S. Chen, X. Yi, and H. Ma, A Novel Method of Fabrication of Micro-Lens Arrays, *Infrared Phys. Technol.*, 2003, **44**, p 133–135
10. M.T. Gale, M. Rossi, J. Pedersen, and H. Schutz, Fabrication of Continuous Relief Micro-Optical Elements by Direct Laser Writing in Photoresists, *Opt. Eng.*, 1994, **22**(11), p 3556–3566
11. K. Zimmer, D. Hirsch, and F. Bigl, Excimer Laser Machining for the Fabrication of Analogous Microstructures, *Appl. Surf. Sci.*, 1996, **96–98**, p 425–429
12. C.C. Chen, M.H. Li, C.Y. Chang, J.K. Sheu, G.C. Chi, W.T. Cheng, J.H. Yeh, and J.Y. Chang, GaN Diffractive Micro-Lenses Fabricated With Grayscale Mask, *Opt. Commun.*, 2003, **215**, p 75–78
13. S.A. Takatsuki, T.Y. Nara, and S.O. Kyoto, Micro-Aspherical Lens and Fabrication Method Therefore and Optical Device, US Patent, 1992, 5,148,322
14. H. Yang, M.C. Chou, A. Yang, C.K. Mu, R.F. Shyu, Realization of Fabricating Micro-Lens Array In Mass Production, *Proceeding of SPIE*, Vol 3739, 1999, p 178–185
15. H. Yang, C.T. Pan, and M.C. Chou, Ultra-Fine Machining Tool/Molds by LIGA Technology, *J. Micromech. Microeng.*, 2001, **11**, p 94–99

16. R. Danzebrink and M.A. Aegerter, Deposition of Optical Microlens Arrays by Ink-Jet Processes, *Thin Solid Films*, 2001, **392**, p 223–225
17. J. Gottert and J. Mohr, Characterization of Micro-Optical Components Fabricated by Deep-Etch X-ray Lithography, *SPIE Micro-Opt. II*, 1991, **1506**, p 170–178
18. T. Okamoto, M. Mori, T. Karasawa, S. Hayakawa, I. Seo, and H. Sato, Ultraviolet-Cured Polymer Microlens Arrays, *Appl. Opt.*, 1999, **38**, p 2991–2996
19. Y.C. Lee and C.Y. Wu, Excimer Laser Micromachining of Aspheric Microlenses with Precise Surface Profile Control and Optimal Focusing Capability, *Opt. Lasers Eng.*, 2007, **45**, p 116–125
20. Y. Fu, Investigation of Microlens Mold Fabricated by Focused Ion Beam Technology, *Microelectron. Eng.*, 2001, **56**, p 333–338
21. W.R. Cox, T. Chen, and D. Hayes, Micro-Optics Fabrication by Ink-Jet Printing, *Opt. Photon. News*, 2001, **12**(6), p 32–35
22. G.H. Kim, A PMMA Composite as an Optical Diffuser in a Liquid Crystal Display Backlighting Unit (BLU), *Eur. Polym. J.*, 2005, **41**, p 1729–1737
23. G.H. Kim, W.J. Kim, S.M. Kim, and J.G. Son, Analysis of Thermo-Physical and Optical Properties of a Diffuser Using PET/PC/PBT Copolymer in LCD Backlight Units, *Displays*, 2005, **26**, p 37–43
24. J.G. Chang and Y.B. Fang, Feasibility Study of Edge-Lit Backlight of Dual-Panel Display by a Simple Configuration Model, *Displays*, 2008, **29**, p 285–296
25. N.F. Borrelli, Efficiency of Microlens Array for Projection LCD, *IEEE*, 1994, **94**, p 338–345
26. P. Heremans, J. Genoe, M. Kuijk, R. Vounckx, and G. Borghs, Mushroom Microlenses: Optimized Microlenses by Reflow of Multiple Layers of Photoresist, *IEEE Photon Technol Lett*, 1997, **9**, p 1367–1369
27. Y.C. Chang, T.H. Hung, H.M. Chen, J.C. Huang, T.G. Nieh, and C.J. Lee, Viscous Flow Behavior and Thermal Properties of Bulk Amorphous $Mg_{58}Cu_{31}Y_{11}$ Alloy, *Intermetallics*, 2007, **15**, p 1303–1308
28. O.N. Senkov, J.M. Scott, and D.B. Miracle, Composition Range and Glass Forming Ability of Ternary Ca–Mg–Cu Bulk Metallic Glasses, *J. Alloys Compd.*, 2006, **424**, p 394–399
29. W.Y. Liu, H.F. Zhang, Z.Q. Hua, and H. Wang, Formation and Mechanical Properties of $Mg_{65}Cu_{25}Er_{10}$ and $Mg_{65}Cu_{15}Ag_{10}Er_{10}$ Bulk Amorphous Alloys, *J. Alloys Compd.*, 2005, **397**, p 202–206
30. Z.P. Lu, C.T. Liu, and Y. Li, Glass Transition and Crystallization of Mg–Ni–Nd Metallic Glasses Studied by Temperature-Modulated DSC, *Intermetallics*, 2004, **12**, p 869–874
31. G. Yuan, T. Zhang, and A. Inoue, Structure and Mechanical Properties of $Mg_{85}Cu_5Zn_5Y_5$ Amorphous Alloy Containing Nanoscale Particles, *Mater. Lett.*, 2004, **58**, p 3012–3016
32. G. Yuan and A. Inoue, The Effect of Ni Substitution on the Glass-Forming Ability and Mechanical Properties of Mg–Cu–Gd Metallic Glass Alloys, *J. Alloys Compd.*, 2005, **387**, p 134–138
33. C.T. Pan and C.H. Su, Fabrication of Gapless Triangular Micro-Lens Array, *Sens. Actuators*, 2007, **134**, p 631–640
34. G.C. Papanicolaou, D. Bakos, and K. Imielinska, Effect of Interfacial Phenomena on the Thermal Expansion Behavior of Rubber-Toughened PMMA Composites, *J. Macromol. Sci. Phys.*, 1998, **37**, p 201–217